

FSEC Solar Cooker Design

Optical Ray Trace Analysis

Ross McCluney

1/24/01

Introduction

The task is to create a model for the cooker's primary mirror, cooking pot with hemispherical bottom, and transparent cover, and then to use computerized ray tracing software ASAP from Breault Research Organization to determine the effectiveness of the basic optical design. This includes a sensitivity analysis of the consequences of changes in the angle of the sun, position of the pot relative to the primary, and other factors, on the concentration of rays on the pot, on the distribution of solar heating over the pot surface, and on the optical losses and their mechanisms.

The optical design provided was of a 1 m² concentrating spherical mirror adjusted by hand every hour or so to point the mirror toward the sun, keeping reflected sun rays on the cooking pot, suspended on a tripod near the focus of the mirror.

Geometry Simulated

Initially it was assumed that the cooking pot will be composed of a hemispherical bottom and a cylindrical top with the following dimensions.

Hemisphere radius = 7.5 cm

Hemisphere diameter = 15 cm

Cylinder radius = 7.5 cm

Cylinder height = 4 cm

The primary mirror is chosen to be spherical. Other figures can be tested later.

Mirror disk radius = 56.5 cm

Mirror disk diameter = 113.0 cm

Mirror disk area = $B r^2 = B (.565 \text{ m})^2 = 1.0 \text{ m}^2 = 10,000 \text{ cm}^2$

Mirror radius of curvature = 200 cm

Mirror approximate focal length = 100 cm

The center of the pot is set initially to be 90 cm from the mirror, a 10 cm displacement in the Z-direction, toward the mirror, from the approximate focal point.

ASAP was set up to default with the above dimensions, and, for the time being, a perfect reflectance of

1.0 for the mirror and a perfect absorptance of 1.0 for the pot. The “inr” file which sends commands to ASAP was set up to prompt for the tilt angle of the pot relative to the spherical mirror. It was easier to tilt the pot than rotate the mirror and the simulated solar source to different solar altitude angles, but optically they are equivalent. The tilt angle shown in subsequent plots is the zenith angle of the mirror axis, the angle of this axis from straight up.

Sensitivity Analysis

The current inr file has an option for positioning the pot along the Z-axis, the axis through the center of and normal to the primary mirror. It is positioned a distance Z (cm) from the zero or origin of the coordinate system, located at exactly 100 cm from the vertex of the mirror, precisely half the mirror’s radius of curvature, the nominal focal point of the mirror. This positioning of the pot is measured from the origin along the Z axis to the center of curvature of the pot bottom. The pot is then rotated about a line parallel to the X-axis through the center of curvature of the pot bottom. The geometry and

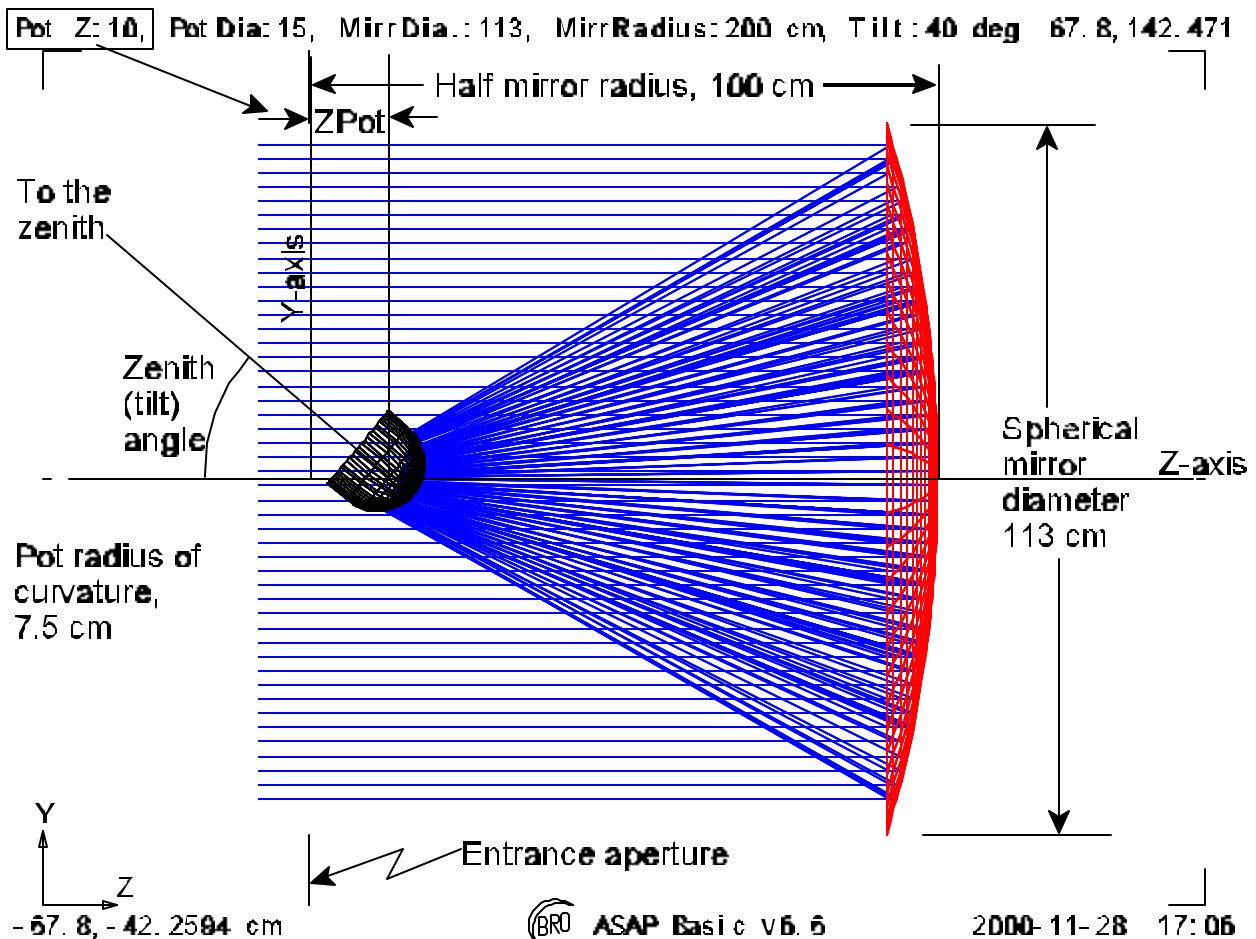


Figure 1. Illustration of the output of an ASAP ray trace. Incident rays (in blue) from the left are reflected from spherical mirror (in red) on the right and converge onto a black absorbing cooking pot (in black) near the origin of the coordinate system. As shown here, the pot is 10 cm to the right of the origin, which is also the approximate focal point for the mirror.

coordinate system is shown in Fig. 1. This drawing was output from ASAP and then annotated in Word Perfect Presentations.

Incident rays, currently shown as absolutely parallel, are incident from the left upon the spherical mirror to the right, are reflected from this mirror back to the left and onto the bottom and side of the cooking pot, the axis of which points toward the zenith. The *inr* file, when run in ASAP, prompts for four parameters:

1. The displacement Z_{pot} of the pot toward the mirror.
2. The tilt of the pot from the axis of the mirror, around an axis through the center of curvature of the pot's bottom.
3. Whether the ray trace is to be performed with relatively few rays, as shown in Fig. 1, to enable visual observation of the ray trajectories, or with a large number of them to improve the smoothness and accuracy of the computed flux distribution incident on the pot.
4. Whether the ray trace is to be performed with a regular grid of parallel rays on a rectangular, equally spaced grid, or with a solar simulator. The latter emits rays randomly from a disk simulating the solar disk at the focus of a large parabolic mirror. The rays from this emitting disk are quasi-collimated by the mirror and sent relatively parallel to the Z -axis onto the primary mirror of the solar cooker. The emitting disk at the focus of the parabola is made to be of such a size that its rays, after reflection from the parabola, will spread over a half degree diameter conical solid angle, thereby simulating the spread of rays from the half degree diameter solar disk.
5. Whether the primary mirror of the cooker is spherical or paraboloidal. The latter was included because some have suggested that a paraboloidal mirror would be superior.

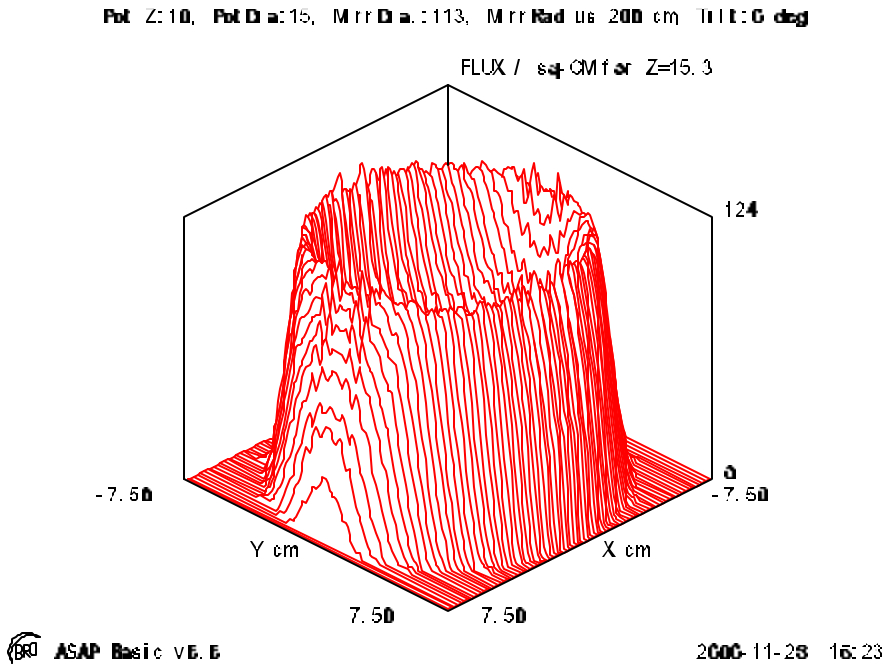


Figure 3. Isometric three dimensional plot of irradiance over the bottom hemispherical area of the pot, projected onto a plane perpendicular to the axis of the pot.

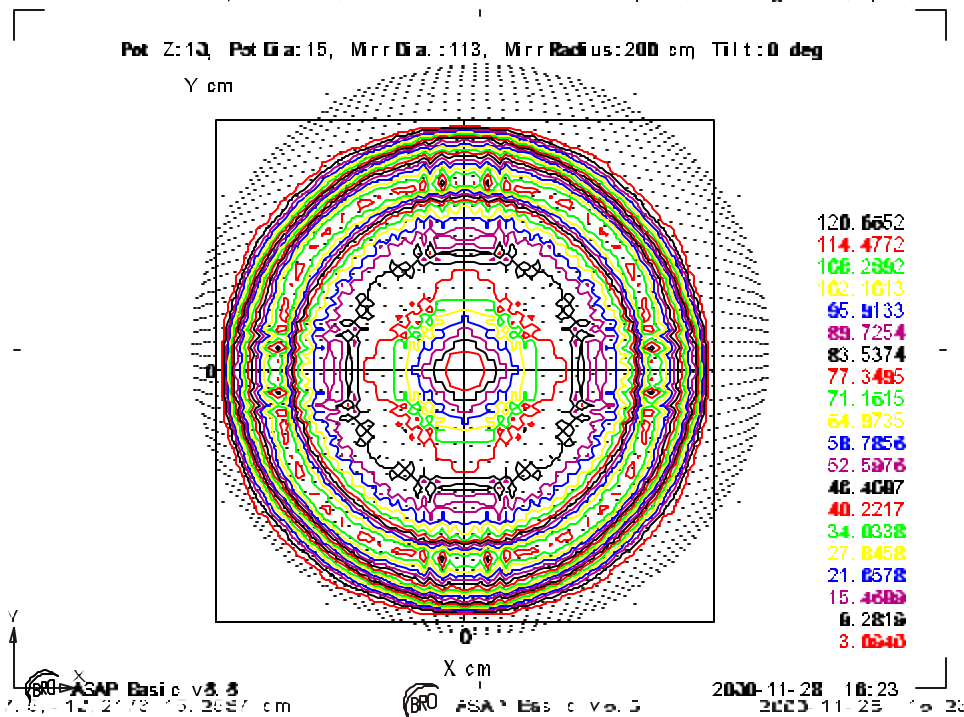


Figure 2. Spot diagram showing ray intersections with the bottom of the cooking pot. **Figure 4.** Contour plot of flux distribution over the bottom of a cooking pot in a solar cooker with the sun directly overhead, at the zenith. The drawing shows a projection of these intersection points onto a plane at the $Z = 15.2587$ cm position.

Initially, the number of rays involved in the few/many simulations are as follows:

Few rays case: 31,428 rays

Many rays case: 196,364 rays

Following are some example results from a series of ray traces with Zpot set to 10 cm.

First, in Fig. 2, is what is called a “spot diagram,” a depiction of the locations on the bottom of the pot where the rays reflected from the mirror impinge upon the hemispherical pot bottom. The hole in the middle of this array represents the shadow of the pot on the mirror, as reflected onto the pot bottom.

In Fig. 3 is shown an isometric plot of the irradiance distribution over the pot bottom. It is clear that the flux is higher near the edges of the 7.5 cm diameter pot than at

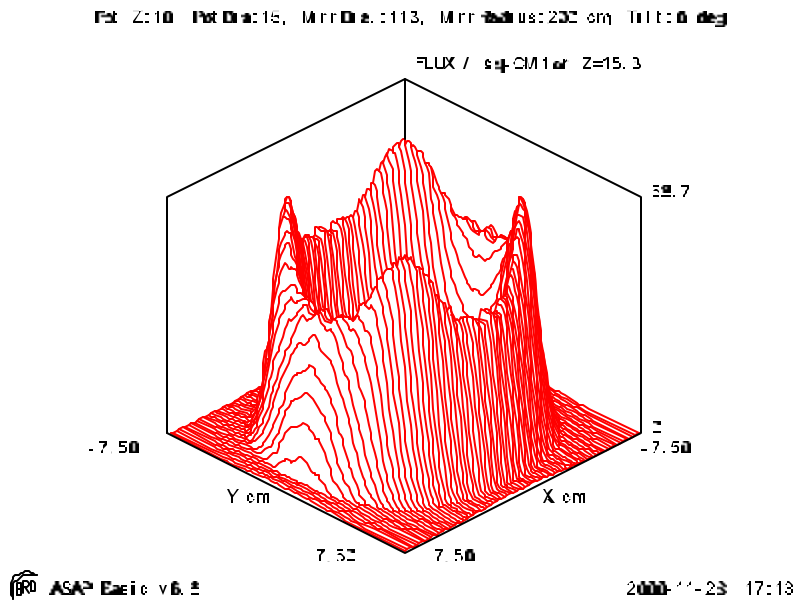


Figure 5. High resolution isometric plot of the irradiance on the bottom of the cooking pot, projected onto a plane perpendicular to the axis of the cylindrical side of the pot.

the middle. This may to some extent be an artifact of the increasing density of rays around the edges of the projection of the pot bottom onto a plane.

The effect is shown more dramatically in Fig. 4, a contour plot of the flux distribution with 20 levels of irradiance plotted.

Running this case in the “many rays” case results in the isometric and contour plots shown in Figs. 5 and 6. The improved “smoothness” of the plot is evident in these figures.

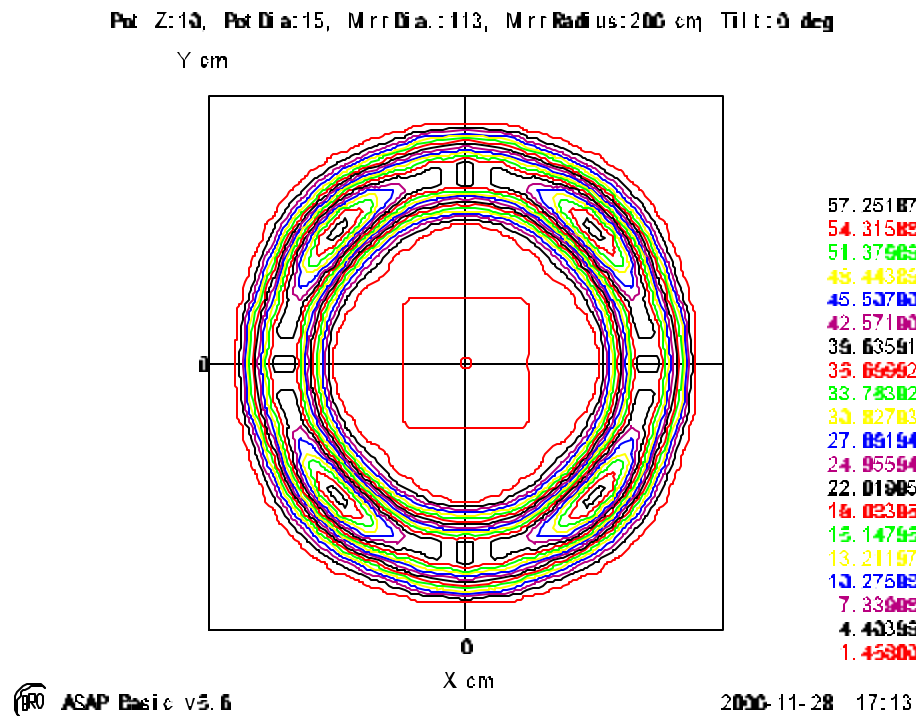


Figure 6. High resolution contour plot of irradiance over cooking pot bottom with sun at the zenith.

Rotation and Displacement.

Before looking at the question of how to obtain a more appropriate map of the flux across the bottom of the pot, rather than a projection onto a plane, we turn to the cases of rotating and displacing the cooking pot.

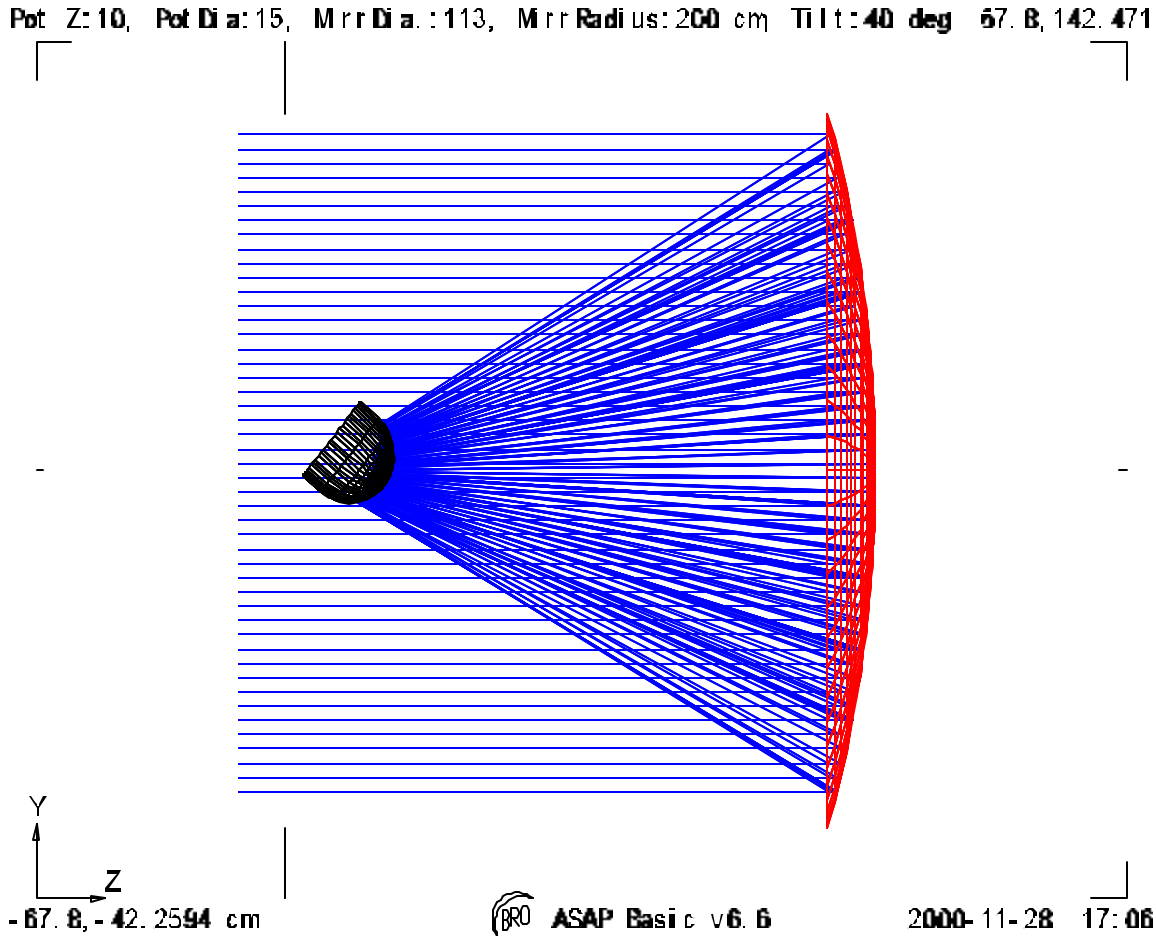


Figure 7. A pot tilt of forty degrees is shown in profile view. Clearly all reflected rays hit the pot, though a fraction impinge on the cylindrical side.

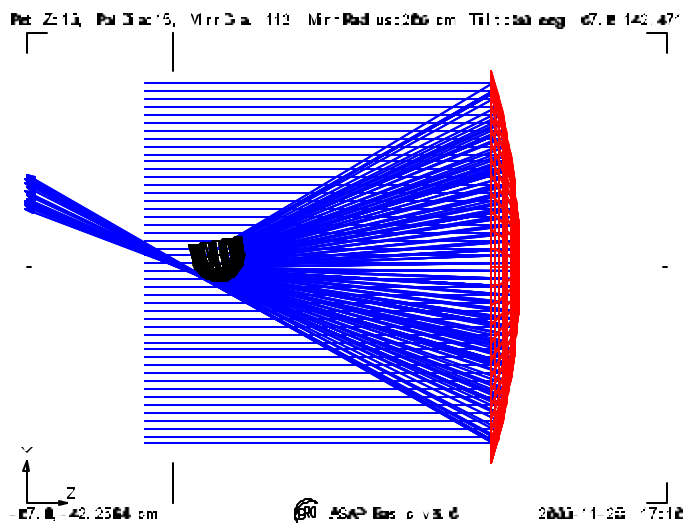


Figure 8. Profile ray trace for tilt angle of 80 degrees.

From the plots shown in Figures 1 through 6, it appears that the 10 cm location is fairly close to the optimum. We'll see the effect of rotating the current pot design and then we'll see how changes in the pot's z-axis location affect the outcome, in this case looking only at the ray trace profile plots.

First is a forty degree tilt, shown in Fig. 7. The rays appear to be fairly uniformly distributed over the pot, including a few on the cylindrical side.

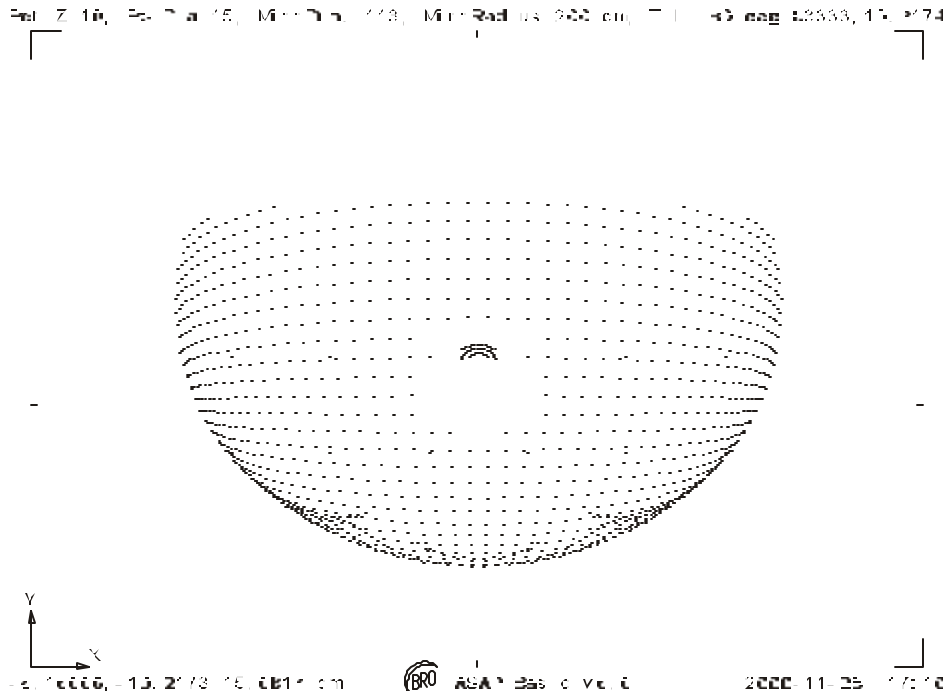


Figure 9. Spot diagram for pot tilted to 80 degrees, showing rays entering the top of the pot and being absorbed inside.

The next plot shows the pot tilted at 80 degrees. This would be for a solar altitude angle of 10 degrees (90 minus 80). At this extreme angle, a few rays miss the pot entirely, and several enter the top of the pot and are absorbed inside. If the pot were full of food, these rays would be intercepted by the food and might experience some scorching. Extending the cylindrical side from 4 cm to 5 or 6 cm should solve this problem, if

indeed it is a problem. (The food would be expected to intercept the rays before they are focused and the transparent top of the pot could easily be given a roughened surface, producing scattering and more even distribution of rays entering the pot through it.) The spot diagram of Fig. 9 shows the concentration of rays after traveling over the lip of the pot and impinging on the opposite side inside the pot.

Solar Simulator

In order to illuminate the system with rays not perfectly parallel but more representative of those emanating from the whole solar disk having an angular diameter of 0.5 deg, a solar simulator was constructed, consisting of a small emitting disk, emitting its rays to the left, at the focus of a paraboloidal mirror reflecting these rays to the right toward the solar cooker. A ray trace and profile plot of this arrangement is shown in Fig. 10.

Hemispherical Map of Pot Irradiance

The isotropic and contour plots of irradiance on the pot bottom given above show an apparent but artificial concentrating of the flux around the edges of the pot. This is an artifact of the projection of flux values from the hemispherical surface onto a plane perpendicular to the Z-axis. The spot diagrams illustrate that ray intersections approximately uniformly distributed over a hemispherical surface, upon linear projection onto a plane will have nonuniform distribution. ASAP offers another way of visualizing flux distributions that may be more appropriate. Since the bottom is spherical, if we analyze the flux

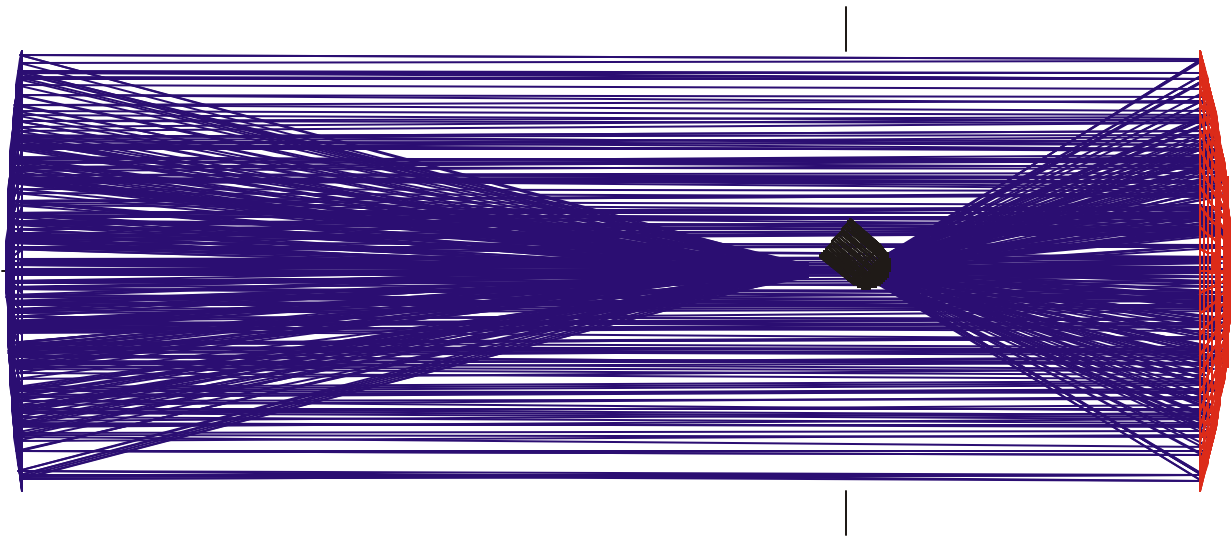


Figure 10. Ray trace and profile plot of solar cooker illuminated with rays from a solar simulator. The simulator consists of a small emitting disk near the center of the plot, sending its rays to the left onto a mirror having the shape of a paraboloid of revolution. The disk is at the focal plane of the mirror, so the reflected rays propagating to the right are quasi-collimated. Their angular spread is set by the size of the emitting disk and the focal length of the parabola to match the 0.5 degree angular spread of rays from the solar disk.

distribution as a function of the angles from and around the z-axis, the result will provide an approximate map of the true flux distribution over the hemispherical bottom.

The remaining intensity plots in this report were obtained in this manner. They give the angular distribution of flux in the rays incident upon the pot. This is not necessarily the same as the spatial irradiance distribution over the pot surface, unless there is a one-to-one mapping of the directions and spatial positions of the rays over the pot surface. From the ray trace profile plots to be shown subsequently, this mapping is approximately correct, but not perfect. To get more accurate mapping will require considerable more work, work considered unnecessary at this stage.

Resetting the Geometry

Preparatory to performing a number of ray traces and in order to ensure that the pot has a capacity close to a liter by volume, the pot was slightly resized, and the length of the cylindrical section was extended to help prevent the sun's rays from entering the interior. With these and other changes, the dimensions for the remaining ray trace analyses are given below.

Primary mirror: Section of a spherical reflector, approximately 1 m².

If $BR^2 = 1$ $R^2 = 1/B = 0.3183$. $R = 0.56$ m, 56 cm, 560 mm

Diameter $D = 1.12$ m or 112 cm

Radius approximately $2L$, so focus distance . L

Let $2L = 200$ cm, so $L = 100$ cm

Pot size: 1 liter desired

Diameter d , height h , tilt θ , distance L from mirror vertex

If $d = 12$ cm, $r = 6$ cm, $h = 8$ cm, then $V_{\text{sph}} = \frac{4}{3} B r^3 = 904 \text{ cm}^3 / 2 = 452 \text{ cm}^3$.

$$V_{\text{cyl}} = B r^2 h = 628$$

$V_{\text{tot}} = V_{\text{sph}} + V_{\text{cyl}} = 1,080 \text{ cm}^3 = 1.08$ liter, close to desired.

Sun straight up, area intercepted by pot = $B r^2 = B(36) = 113 \text{ cm}^2$

Area intercepted by mirror = 1 m^2 Pot-to-mirror area ratio = 0.113 or 11.3%.

Concentration ratio averaged over whole pot bottom, sun straight up = 8.84.

Pot location: 8 cm toward mirror from focus at L , call it $Z_{\text{pot}} = L - 8$ cm.

Geometric efficiency is defined to be the ratio of flux received by the pot to the total flux contained in all the rays from the source, without losses due to reflection, scattering, or absorption. If all the rays launched terminate on the pot, the geometric efficiency would be 100%. Commands were added to the *inr* file to calculate the geometric efficiency for each ray trace. The calculated values ranged from 98.83% to 99.96% for all the cases run, indicating efficient optical design, with the pot capturing nearly all the rays reflected from the primary mirror.

Ray Trace Results

A series of ray traces were performed, with varying inputs, to test the sensitivity of the optical system to a variety of changes. First the Z -position of the blackened pot was set at 4 cm from the best focus position, causing the pot to intercept converging rays from the mirror before they reach the focus. The zenith angle was set to zero. Then ray traces were performed with few (31,428) versus many (196,364) rays launched, with a spherical primary mirror and a paraboloidal one, and with a solar simulator versus a simple grid of precisely parallel rays.

Even in the few rays case, if every ray were shown in the profile plots, they would be completely filled from so many rays. ASAP has an option, however, for plotting only a fraction of the rays actually launched and used for the calculations. The ray trace results for these four comparison cases are shown in Figs. 11, 12, 13 and 14. The process of sampling the rays launched in a regularly spaced grid, as illustrated in Fig. 1, in the case of many rays means that only selected rays are plotted, and these do not fall on a regular grid but appear to be randomly distributed spatially. These and all remaining Figures are placed at the end of this report.

The corresponding isometric and contour plots are shown in Figs. 15, 16, 17, and 18 and in Figs. 19, 20, 21 and 22, respectively. It appears that the parabolic mirror case shown in Fig. 13 produces a larger spread of the rays reaching the pot bottom. However, looking at the isometric and contour plots for this case, there appears to be little difference in the angular spread of the flux in all four cases. Because of this, future simulations are done either with the case of many rays or with few, and with the grid of rays option, and a spherical reflector.

Figures 23 through 25 show profile plots for the pot tilt angle going to 40, 60, and 80 degrees. As long as the rays are received by the pot surface, the isometric and contour plots should be the same for all these, since they plot the angular variation, not the spatial variation over the pot surface. We must infer the spatial distribution of flux from the profile plots. To verify this conclusion, the contour plots corresponding to Figs. 23 through 25 are shown in Figures 26 through 28.

Figures 23 through 25 and 29 through 36 show trace profile results for displacements of 4, 6, and 8 cm and for tilt angles of 0, 40, 60, and 80 degrees. It is seen that in all cases all rays from the mirror are intercepted by the cooking pot, with the exception of the 80 degree case and an 8 cm displacement.

It is clear from these figures that, while the rays nearly all reach the pot and are spread over a moderately large area of it, there is still considerable concentration near the optical axis. In an attempt to spread the rays over a larger area, without losing any by missing the cooking pot, the mirror radius was shortened, keeping the same aperture area of approximately 1 m².

The result is shown in Fig. 37, where the previously 200 cm radius of curvature has been shortened to 100 cm, making the focal length approximately 50 cm. As can be seen from the profile plot of Fig. 37, the rays are spread over a wider area of the pot bottom. To see if any rays miss the pot at the maximum angle of 80 degrees, another trace was performed and the isometric and contour plots were also created. These results are shown in Figures 38, 39, and 40.

Though the new distribution retains the fairly steep drop-off of flux at the edges of the distribution, the central portion is now broader and more constant, with a slight dip in the irradiance on axis. Having the peak solar heating occur in a ring around the center of the distribution should result in more even heating and less chance for food burning at a hot spot.

These results indicate the importance of choosing a metal for the pot having high lateral conductivity, better to spread the heat from the solar focus over the pot surface.

We end up with the following dimensions for the solar cooker design:

Mirror spherical with radius of curvature 100 cm and approximate focal length of 50 cm.

Mirror diameter 112 cm for a mirror area of 0.9852 m².

Spherical bottom cooking pot with 12 cm diameter, 6 cm radius, 44 cm from the mirror vertex to the center of curvature of the bottom.

Pot side cylindrical with diameter 12 cm and height 8 cm.

Pot volume approximately 1 liter.

Glazing and strut losses

The glazing used to admit solar radiation while reducing conductive, convective, and radiative losses of heat from the pot will introduce some losses of incident solar flux, due to reflection, scattering, and

deviation of the rays from striking the pot, but with a good design these losses should be slight. The shadowing action of the support struts likewise will reduce efficiency slightly. The magnitudes of these losses should not be difficult to estimate. Determining the geometrical area of the mirror obscured by the struts should yield a loss factor, the fraction of mirror area obscured. The transmittance of the glazing material should provide a second loss factor. If the glazing geometry is such that rays from the mirror approaching the cooking pot are incident on the glazing over a range of angles of incidence, then the transmittance of the material alone will be insufficient for estimating losses from this source. Additional ray tracing can be used to assess the magnitudes of these losses if the geometry of the glazing is known precisely and the refractive index, absorptance, and scattering coefficient of the glazing material are provided.

Figures

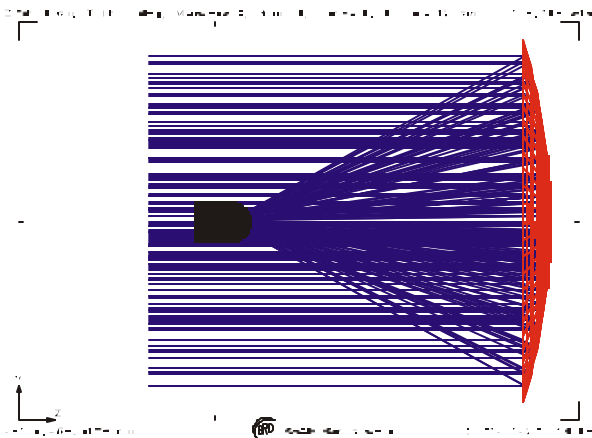


Figure 11. Ray trace profile plot for the case of few rays, parallel grid of incident rays, and a spherical mirror.

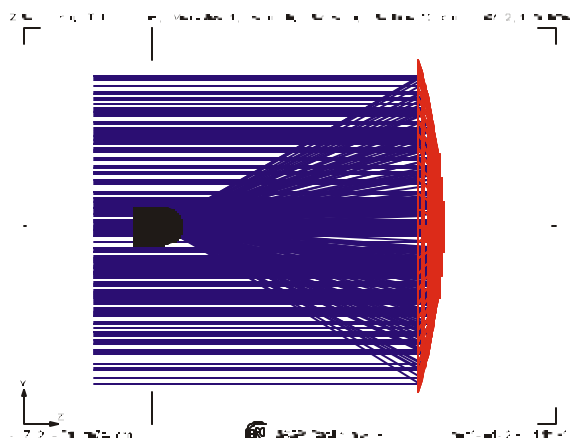


Figure 12. Ray trace profile for many rays, parallel grid of incident rays, and spherical mirror.

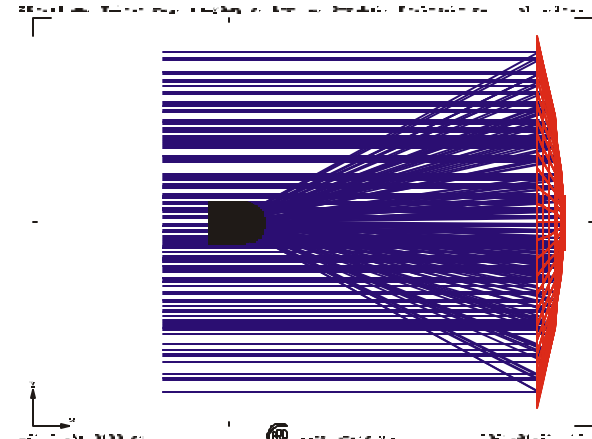


Figure 13. Ray trace profile for few rays, parallel grid, and parabolic mirror.

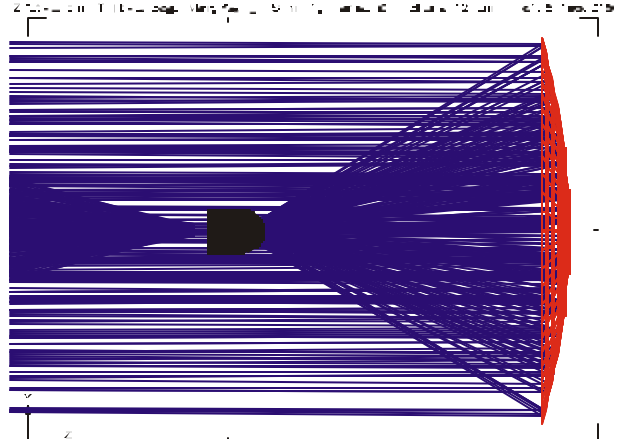


Figure 14. Ray trace profile for few rays, solar simulator and spherical mirror.

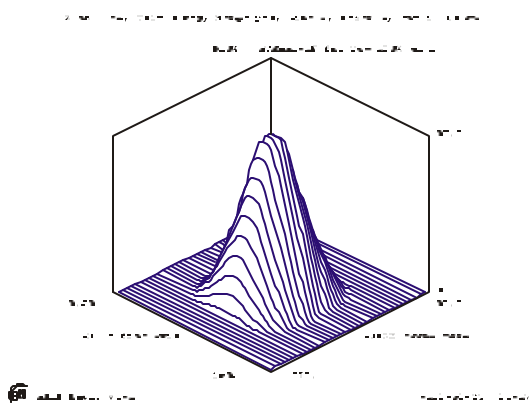


Figure 15. Isometric plot of ray flux versus polar angles. Few rays, parallel grid and spherical mirror

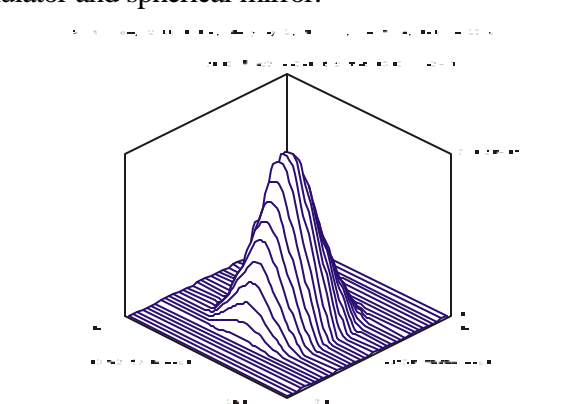


Figure 16. Isometric plot for many rays, parallel grid and spherical mirror.

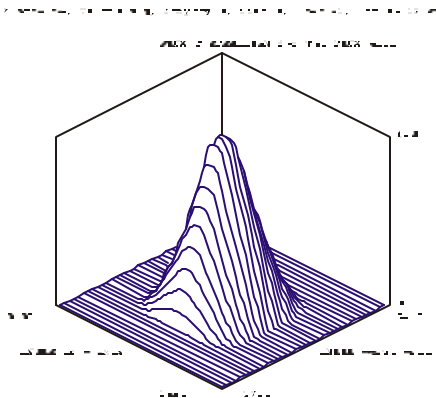


Figure 17. Isometric plot for few rays, parabolic mirror, and grid of rays.

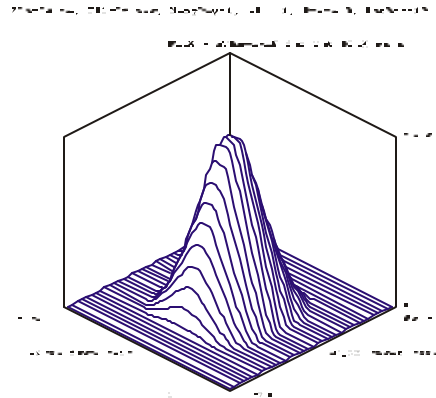


Figure 18. Isometric plot for many rays, spherical mirror, and solar simulator.

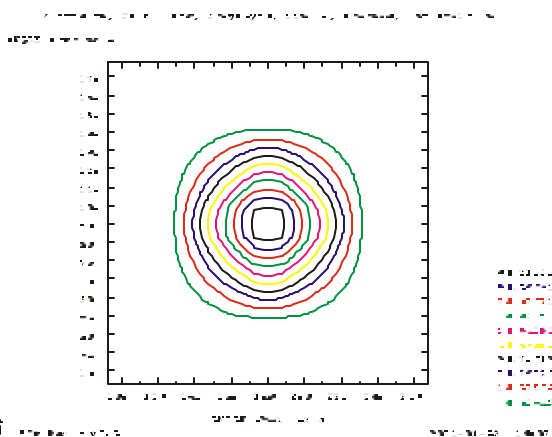


Figure 19. Contour plot of rays on cooking pot for few rays case, spherical mirror, and grid of rays as source.

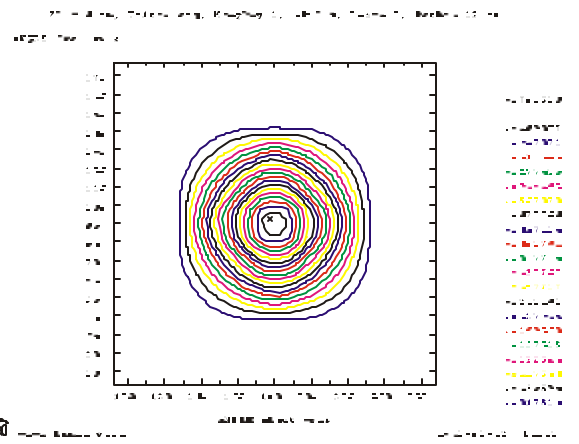


Figure 20. Contour plot for many rays case, spherical mirror, and grid source.

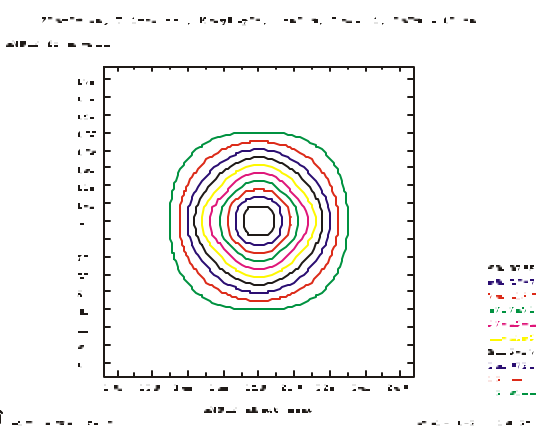


Figure 21. Contour plot for few rays case, paraboloidal mirror, grid source.

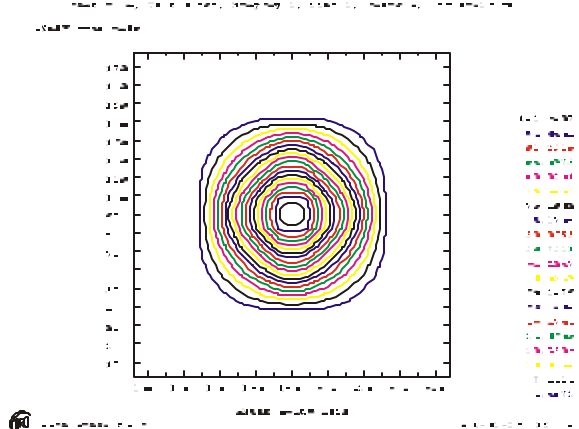


Figure 22. Contour plot for many rays, spherical mirror, and solar simulator.

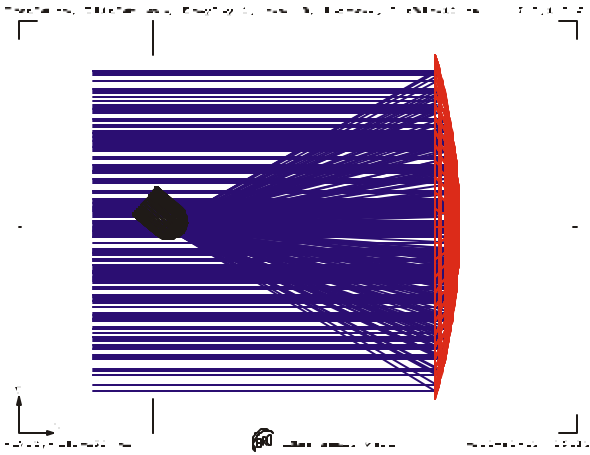


Figure 23. Ray trace profile for 4 cm displacement and tilt angle 40 degrees, spherical mirror, and grid of rays.

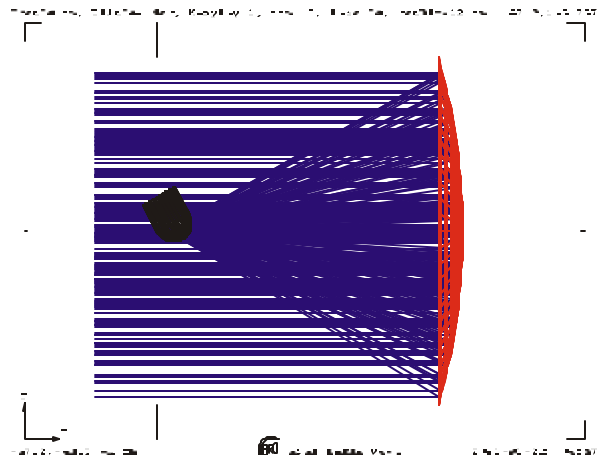


Figure 24. Ray trace profile for 4 cm displacement and tilt angle 60 degrees.

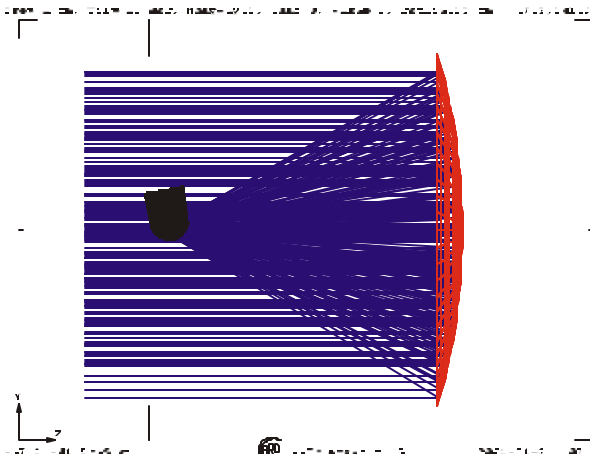


Figure 25. Ray trace profile for 4 cm displacement and tilt angle 80 degrees.

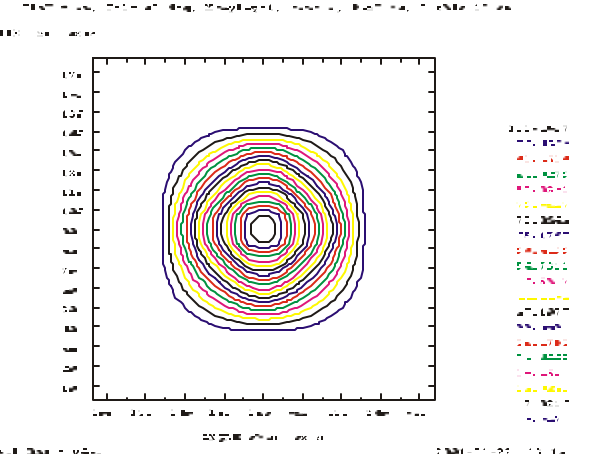


Figure 26. Contour plot for 4 cm, 40 degree tilt, spherical mirror, grid source.

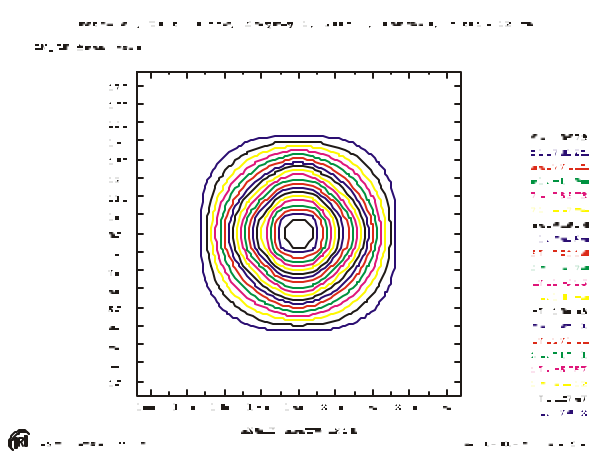


Figure 27. Contour plot for 4 cm, 60 degree tilt, spherical mirror, many rays, grid source.

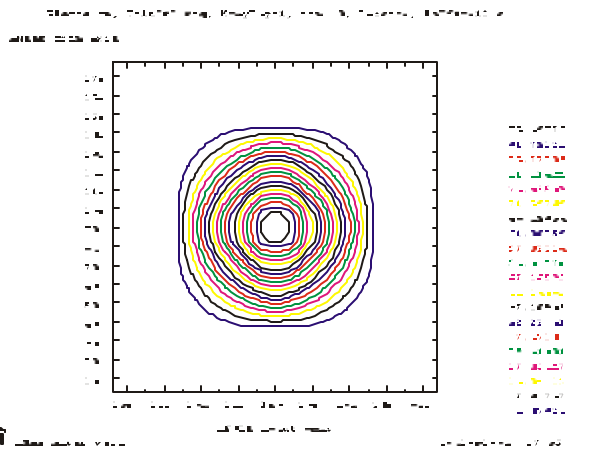


Figure 28. Contour plot for 4 cm, 80 degree tilt, spherical mirror, many rays.

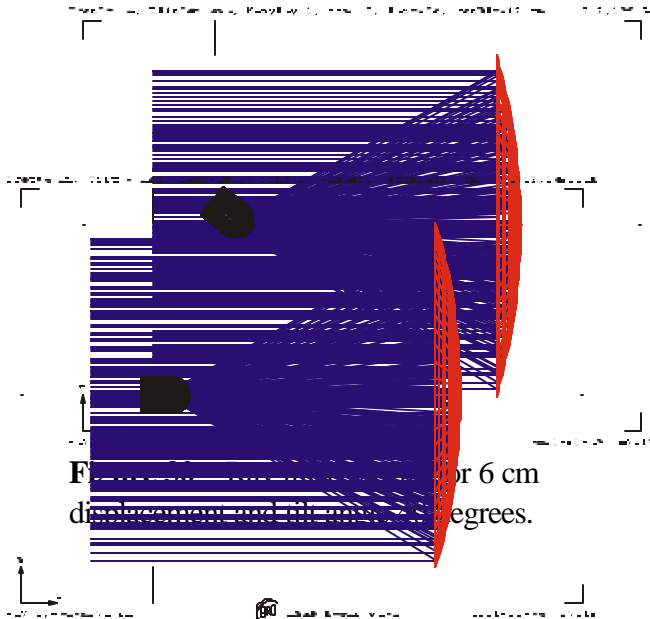


Figure 29. Ray trace profile for 6 cm displacement and tilt angle 0 degrees.

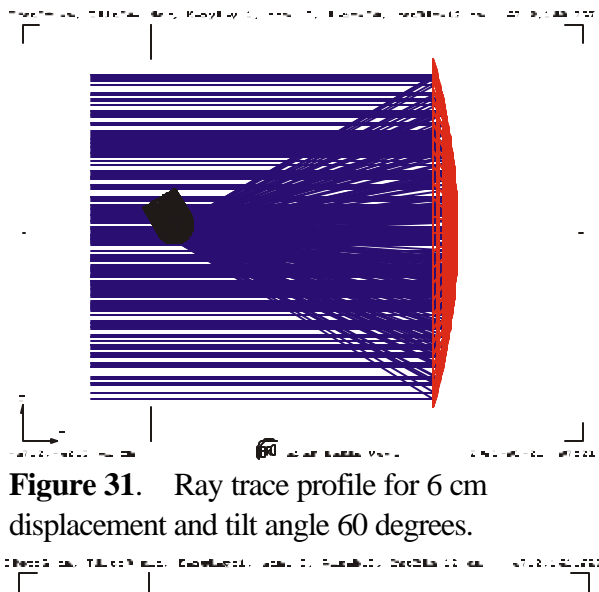


Figure 31. Ray trace profile for 6 cm displacement and tilt angle 60 degrees.

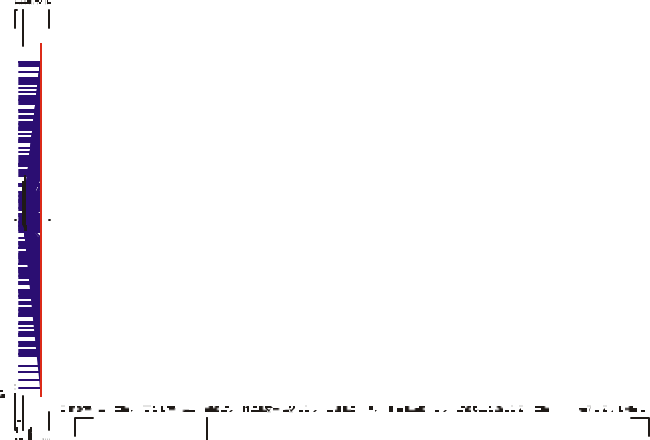


Figure 32. Ray trace profile for 6 cm displacement and tilt angle 80 degrees.

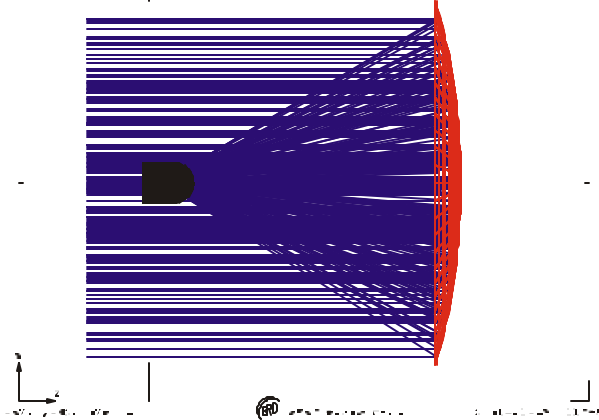


Figure 33. Ray trace profile for 8 cm displacement and tilt angle 0 degrees.

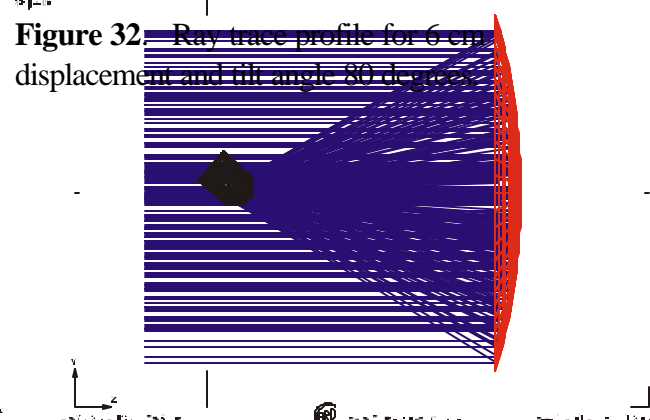


Figure 34. Ray trace profile for 8 cm displacement and tilt angle 40 degrees.

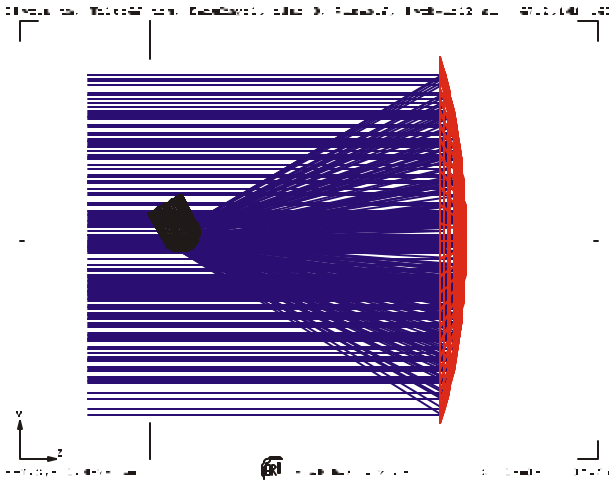


Figure 35. Ray trace profile for 8 cm displacement and tilt angle 60 degrees.

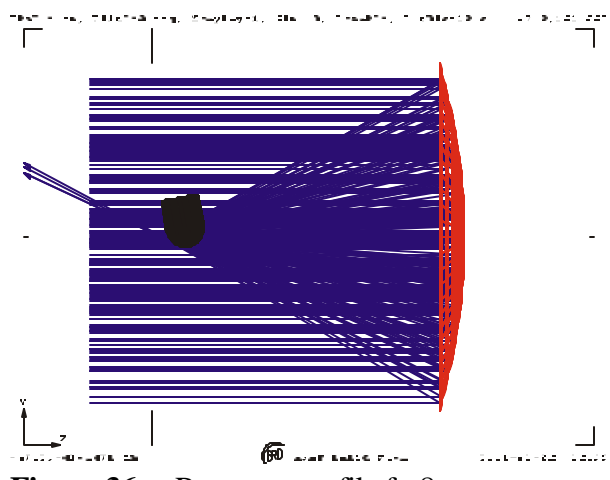


Figure 36. Ray trace profile for 8 cm displacement and tilt angle 80 degrees.

ZDists: 6 cm, Tilt: 0 deg, ManyRay: 0, Size: 0, Parab: 0, PotDist: 12 cm 51.2, 96.4188

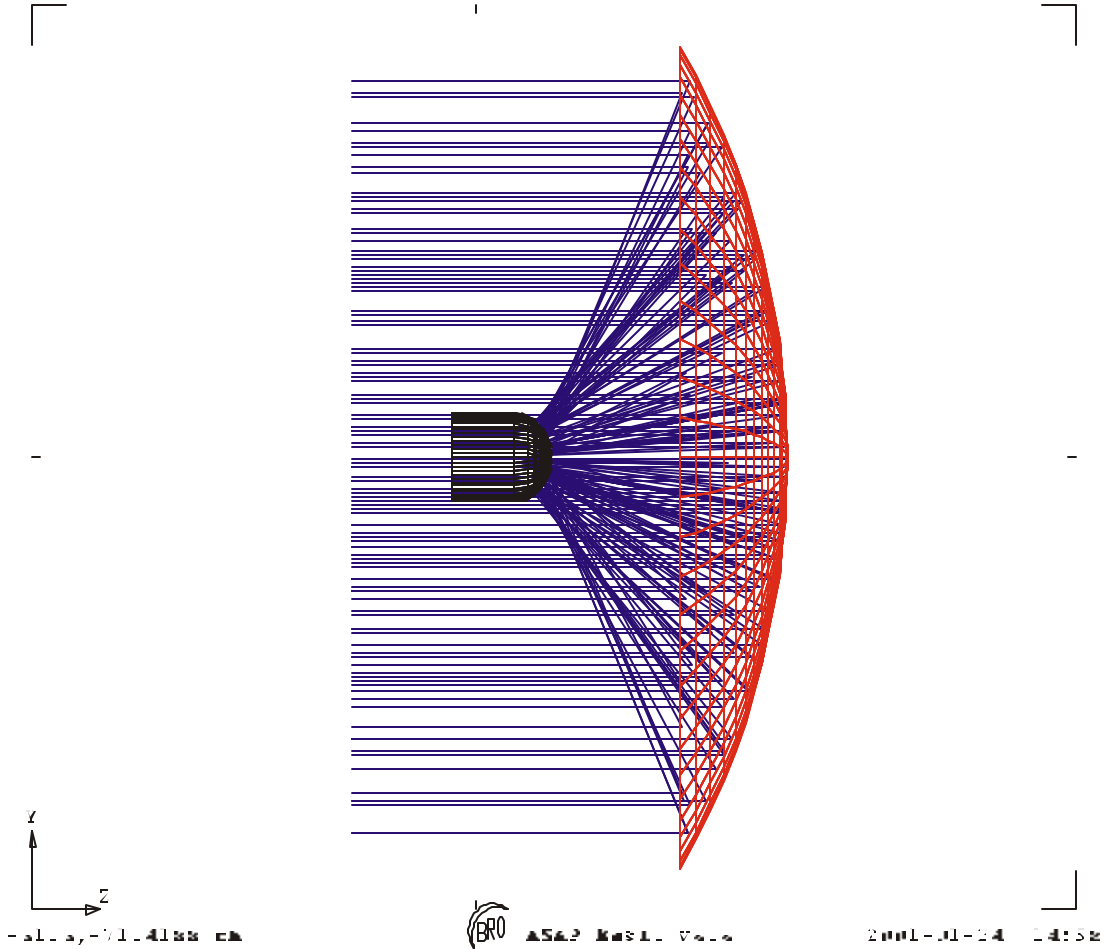


Figure 37. Ray trace profile for 6 cm displacement, tilt angle 0, and 50 cm focal length.

ZPot:5 cm, Tilt:80 deg, ManyRay:0, Size: 7, Parabola, PotDiam:10 cm 51.5,59.4122

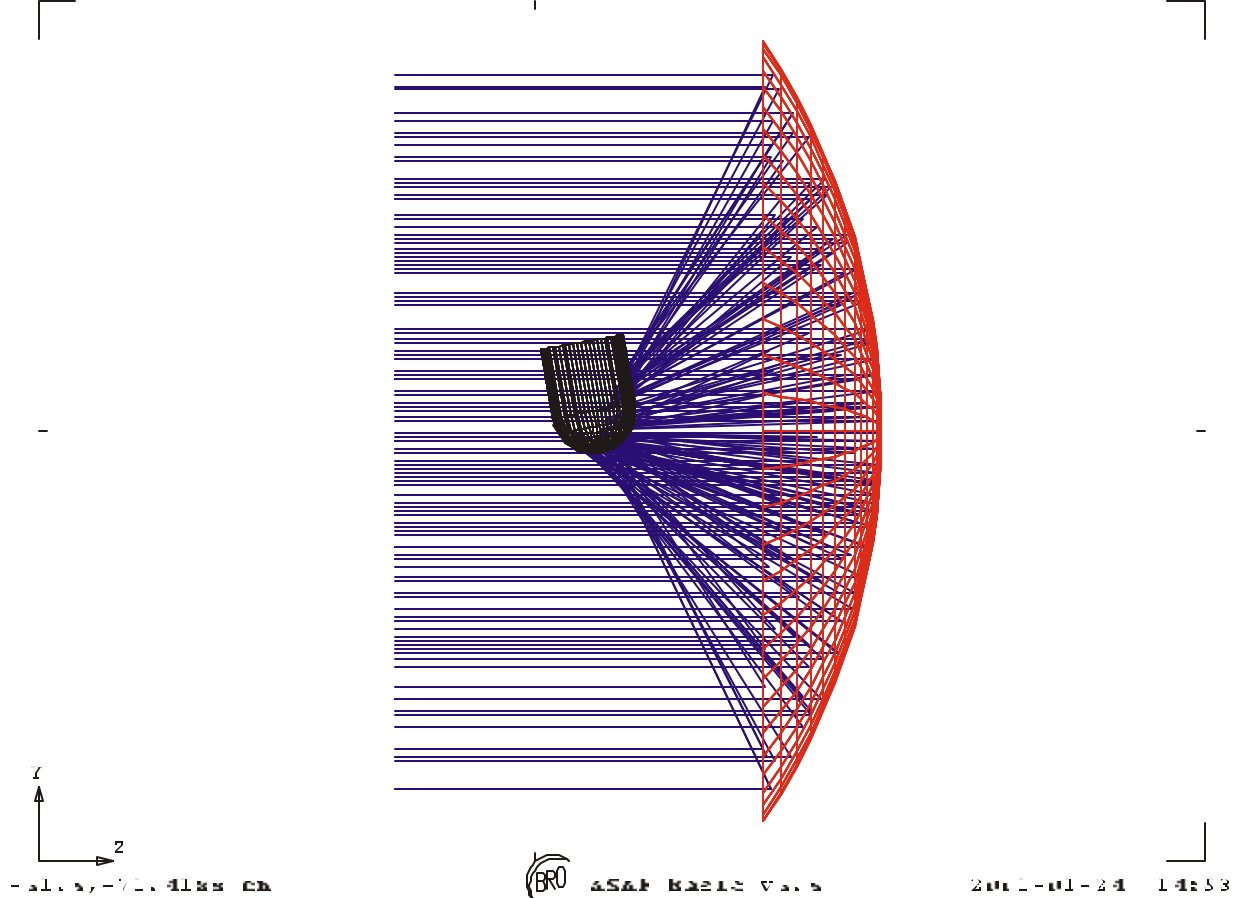


Figure 38. Ray trace profile plot of 100 cm radius mirror and pot tilted at 80 degrees. Mirror area is still approximately 1 sq. m.

ZPot:5 cm, Tilt:80 deg, ManyRay:0, Size: 7, Parabola, PotDiam:10 cm
ASAP R2212 V3.1

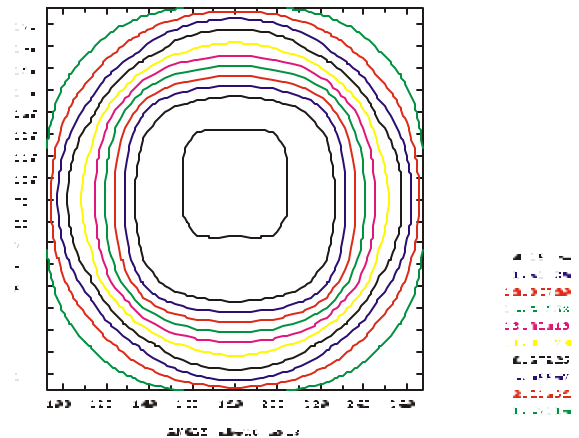


Figure 39. Contour plot of the flux distribution for the system shown in Fig. 35.

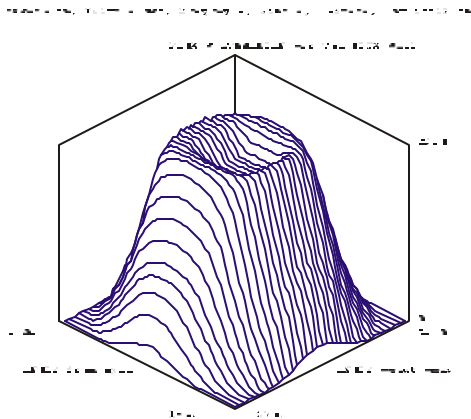


Figure 40. Isometric plot of flux distribution for the system shown in Fig. 35.